



# Maintaining forest cover to enhance temperature buffering under future climate change

Emiel De Lombaerde<sup>a,\*</sup>, Pieter Vangansbeke<sup>a</sup>, Jonathan Lenoir<sup>b</sup>, Koenraad Van Meerbeek<sup>c</sup>, Jonas Lembrechts<sup>d</sup>, Francisco Rodríguez-Sánchez<sup>e</sup>, Miska Luoto<sup>f</sup>, Brett Scheffers<sup>g</sup>, Stef Haesen<sup>c</sup>, Juha Aalto<sup>h</sup>, Ditte Marie Christiansen<sup>i</sup>, Karen De Pauw<sup>a</sup>, Leen Depauw<sup>a</sup>, Sanne Govaert<sup>a</sup>, Caroline Greiser<sup>i</sup>, Arndt Hampe<sup>j</sup>, Kristoffer Hylander<sup>k</sup>, David Klimes<sup>l</sup>, Irena Koelemeijer<sup>i</sup>, Camille Meeussen<sup>a</sup>, Jerome Ogée<sup>m</sup>, Pieter Sancier<sup>a</sup>, Thomas Vanneste<sup>a</sup>, Florian Zellweger<sup>n</sup>, Lander Baeten<sup>a</sup>, Pieter De Frenne<sup>a</sup>

<sup>a</sup> Forest and Nature Lab, Ghent University, Ghent, Belgium

<sup>b</sup> Ecologie et dynamique des systèmes anthropisés (EDYSAN), UMR CNRS 7058, Amiens, France

<sup>c</sup> Department of Earth and Environmental Sciences, KU Leuven, Leuven, Belgium

<sup>d</sup> Research Group Plants and Ecosystems, University of Antwerp, Wilrijk, Belgium

<sup>e</sup> Dept. Biología Vegetal y Ecología, Universidad de Sevilla, Sevilla, Spain

<sup>f</sup> Department of Geosciences and Geography, University of Helsinki, Helsinki, Finland

<sup>g</sup> Department of Wildlife Ecology and Conservation, University of Florida, Gainesville, United States

<sup>h</sup> Weather and Climate Change Impact Research, Finnish Meteorological Institute, Helsinki, Finland

<sup>i</sup> Department of Ecology, Environment and Plant Sciences, Stockholm University, Stockholm, Sweden

<sup>j</sup> BIOGECO, INRAE, Univ. Bordeaux, Cestas, France

<sup>k</sup> Department of Ecology, Environment and Plant Sciences, Bolin Centre for Climate Research, Stockholm University, Stockholm, Sweden

<sup>l</sup> School of Natural Resources and Environment, University of Florida, Gainesville, United States

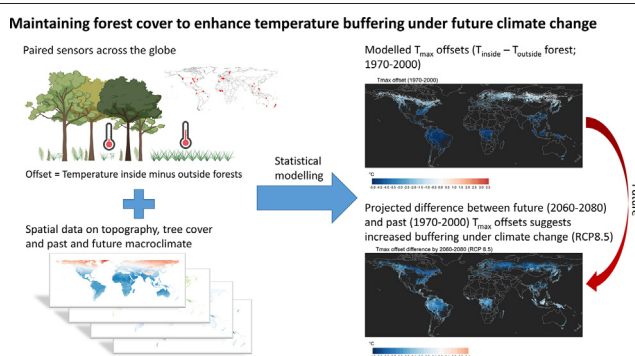
<sup>m</sup> INRAE, Bordeaux Science Agro, ISPA, Villenave d'Ornon, France

<sup>n</sup> Swiss Federal Institute for Forest, Snow and Landscape Research WSL, Birmensdorf, Switzerland

## HIGHLIGHTS

- Temperature differences inside vs. outside forests were mapped across the globe.
- Forest canopies buffer minimum ( $T_{\min}$ ), mean ( $T_{\text{mean}}$ ) and maximum ( $T_{\max}$ ) temperatures.
- In the future, buffering for  $T_{\text{mean}}$  and  $T_{\max}$  may increase, but may decrease for  $T_{\min}$ .
- Refugial capacity of forests might last longer than anticipated in a warming world.

## GRAPHICAL ABSTRACT



## ARTICLE INFO

### Article history:

Received 1 September 2021

Received in revised form 26 October 2021

Accepted 26 October 2021

Available online 5 November 2021

Editor: Elena Paoletti

## ABSTRACT

Forest canopies buffer macroclimatic temperature fluctuations. However, we do not know if and how the capacity of canopies to buffer understorey temperature will change with accelerating climate change. Here we map the difference (offset) between temperatures inside and outside forests in the recent past and project these into the future in boreal, temperate and tropical forests. Using linear mixed-effect models, we combined a global database of 714 paired time series of temperatures (mean, minimum and maximum) measured inside forests vs. in nearby open habitats with maps of macroclimate, topography and forest cover to hindcast past (1970–2000) and to

\* Corresponding author.

E-mail address: [emieli.delombaerde@ugent.be](mailto:emieli.delombaerde@ugent.be) (E. De Lombaerde).

**Keywords:**

Forest microclimate  
Temperature offsets  
Canopy  
Climate change  
Future climate projections  
Paired sensor data

project future (2060–2080) temperature differences between free-air temperatures and sub-canopy microclimates. For all tested future climate scenarios, we project that the difference between maximum temperatures inside and outside forests across the globe will increase (i.e. result in stronger cooling in forests), on average during 2060–2080, by  $0.27 \pm 0.16$  °C (RCP2.6) and  $0.60 \pm 0.14$  °C (RCP8.5) due to macroclimate changes. This suggests that extremely hot temperatures under forest canopies will, on average, warm less than outside forests as macroclimate warms. This knowledge is of utmost importance as it suggests that forest microclimates will warm at a slower rate than non-forested areas, assuming that forest cover is maintained. Species adapted to colder growing conditions may thus find shelter and survive longer than anticipated at a given forest site. This highlights the potential role of forests as a whole as microrefugia for biodiversity under future climate change.

© 2021 Elsevier B.V. All rights reserved.

## 1. Introduction

Warming temperatures and changing precipitation regimes are influencing ecosystems across the globe (IPCC, 2018). To date, ecological research assessing the impact of anthropogenic climate change has predominantly relied on macroclimatic data. These data are typically based on a global network of weather stations established at approximately 1.5 to 2.0 m above the soil surface in open habitats (e.g. above short grass) (World Meteorological Organization, 2018). Forest organisms living below and within tree canopies, however, experience microclimatic conditions distinct from those in open habitats (Chen et al., 1999; De Frenne et al., 2021; Geiger et al., 2009). Below tree canopies, lower radiation, wind and evapotranspiration rates often translate into lower temporal variation in air temperature and humidity compared to open environments (Davis et al., 2019; Geiger et al., 2009; Von Arx et al., 2013). In particular, temperature extremes are often strongly attenuated in forest interiors, with lower maxima and higher minima compared to open environments (De Frenne et al., 2019; Li et al., 2015). Studies have already shown that such microclimatic buffering can mediate the response of forest communities to climate change (De Frenne et al., 2013; Dietz et al., 2020; Lenoir et al., 2017; Stevens et al., 2015; Zellweger et al., 2020). Despite the increasing evidence that ecosystem dynamics and processes are more likely to be related to forest microclimates than to macroclimate (Chen et al., 2018; De Frenne et al., 2021; De Smedt et al., 2021; Frey et al., 2016a), microclimates are still seldom incorporated in ecological research (e.g. in species distribution models) (Lembrechts et al., 2019) and ignored by dynamic global vegetation models (DGVMs; e.g. Thrippleton et al., 2016) that simulate the effects of future climate change on natural vegetation and its carbon and water cycles. In particular, we do not know how forest microclimates will change in the future as macroclimate changes (Lembrechts and Nijs, 2020).

Advances in studies on the effects of climate change on different organisms living below or in forest canopies have often been limited by the availability of suitable microclimatic data (De Frenne et al., 2021). One robust way to study forest microclimates is to use microclimate measurements from paired (inside vs. outside forests) sensor networks to calculate temperature offsets, i.e. the absolute and instantaneous difference between temperature inside (i.e., microclimate) and free-air temperatures outside forests (i.e., macroclimate) (sensu De Frenne et al., 2021). Negative offset values thus reflect cooler and positive offsets warmer forest temperatures compared to outside forests. These empirical offset values for temperature can be related to readily available environmental data using statistical modelling approaches, and these models can then be used to interpolate and extrapolate microclimate across entire mapped landscapes (Frey et al., 2016b; Greiser et al., 2018). Differences between macro- and microclimate (i.e., temperature offsets) result from processes operating at many scales that influence incoming solar radiation, air mixing, soil properties or evapotranspiration (reviewed in De Frenne et al., 2021). Macroclimatic conditions (e.g., mean temperature and rainfall), topographic variation in the landscape (e.g., elevation and aspect) and variation in canopy cover and vegetation height have been reported to be the main drivers of the

understorey temperatures in forests (De Frenne et al., 2019, 2021; Greiser et al., 2018; Macek et al., 2019; Zellweger et al., 2019). With the advent of global forest microclimate data (De Frenne et al., 2019; Zellweger et al., 2020), this type of modelling now enables the prediction of forest microclimates across forest types under future climate change.

Here we map forest microclimate temperature offsets based on (i) paired sensor measurements below the canopy vs. the open-air temperature at a given site and (ii) landscape- and canopy-scale predictors throughout the year for the Earth's dominant forested ecosystems across five continents and at a spatial resolution of ~1 km. More specifically, our objectives were to (1) make predictions for mean, minimum and maximum temperatures using past macroclimatic data (1970–2000), and, (2) make projections for temperature offsets for the future (2060–2080) macroclimatic conditions. We hypothesised that the buffering capacity of forest canopies results in slower future warming of forest below-canopy temperatures compared to the warming observed in standard meteorological weather stations (macroclimate).

## 2. Material & methods

### 2.1. Paired plot data

We used a unique data set with 714 temperature offset data points involving paired plots from 74 studies spread across 5 continents (Supplementary Material Fig. S1; Data available in De Frenne et al., 2019). Focus was on air temperature below tree canopies (~72% of observations) and the temperature of the topsoil (~28%), given their importance for responses of forest organisms and ecosystem functioning to macroclimate warming. A key asset of this database is the paired nature of the data, which always combines below-canopy temperature data at a given forest site with open-air temperature data from a neighbouring reference non-forest site. Temperature measurement were performed by various logger types such as HOBO loggers (~15% of observations), iButton loggers (~10%), full weather stations (~5%) and various other logger types (e.g. cylindrical thermistor, Hanna thermohygrometer, thermocouples, etc.; ~70%). Reference sites were a nearby open site equipped with the same type of (shielded) temperature loggers (~82% of observations), a nearby weather station (~14%) (provided the distance did not conflict with the temperature offset of the canopy, e.g., due to significant topographic differences) or a logger placed above the upper canopy surface (~4%). We specifically refrained from using additional data on forest microclimate conditions that were not strictly paired with free-air conditions from a neighbouring site using the exact same design (same sensor, same logger, same shielding material, same height).

The data points were collated from the scientific literature in a systematic and reproducible manner (see De Frenne et al., 2019 for full details). Temperature offsets were calculated as the temperature inside the forest minus the temperature outside the forest, or extracted directly from the original study; negative values reflect cooler temperatures below tree canopies while positive values reflect warmer

understorey temperatures. This was done for three temperature response variables, i.e. mean, maximum, and minimum temperature (further referred to as  $T_{\text{mean}}$ ,  $T_{\text{min}}$  and  $T_{\text{max}}$ , respectively) that were computed during a specific time period that could differ between sites but that was exactly the same between paired sensors installed outside and inside the forest at a given site. Multiple forest sites (at least several kilometres apart), seasons (meteorological seasons, later aggregated to growing versus non-growing season) and temperature metrics (maximum, mean, minimum, air or soil temperatures) originating from the same study were entered into different rows of the database but tagged under the same study ID. Temperature values of long time series were always aggregated per season and/or year, which means that several temperature values for  $T_{\text{mean}}$ ,  $T_{\text{min}}$  or  $T_{\text{max}}$  could be generated for the same study site. Temperature measurements were classified as having taken place during the growing season, the non-growing season or throughout the whole year. This classification was performed on the basis of reported meteorological seasons and/or climate information in the original study. The dry and winter season were classified as the non-growing season in tropical and temperate biomes, respectively. Estimates of uncertainty (standard error, standard deviation, coefficient of variation or confidence intervals) of the temperature measurements were only reported for a small minority (13.6%) of offset values in the database and were thus not included in our analyses. See De Frenne et al. (2019) for more details on the literature search, inclusion criteria and the empirical data used in this study.

## 2.2. Predictor variables

To predict the offsets for the three temperature variables ( $T_{\text{mean}}$ ,  $T_{\text{max}}$ ,  $T_{\text{min}}$ ) across all forests at a global extent, we gathered global maps of predictor variables related to macroclimate, topography and forest cover. These three sets of predictor variables were selected based on their importance for forest microclimate, and on the spatial resolution and extent of the available data. All the predictor maps we used are raster maps with a spatial resolution of 30 arcsec (~1 km) and are available at the global extent (i.e., from 80°N to 56°S in latitude and from 180°E to 180°W in longitude). Values for all predictor variables were extracted using the geographical coordinates for each plot pair.

### 2.2.1. Macroclimate

Global raster maps of mean, minimum and maximum free-air temperature (°C;  $T_{\text{macro}}$ ), on a monthly basis, as well as monthly precipitation (mm) raster maps, averaged for the climatology 1970–2000, were collected from WorldClim version 2.1 (Fick and Hijmans, 2017). In addition, we gathered future projections (2060–2080) for the exact same set of temperature and precipitation variables described in the previous sentence but based on the contrasting “very stringent” representative concentration pathway (RCP) 2.6 and “worst case” RCP 8.5 from three different general circulation models (GCMs) with minimal interdependency, based on Sanderson et al. (2015), i.e. HadGEM2-ES, MPI-ESM-LR and MIROC5 (downscaled CMIP5 data from WorldClim; 30 arcsec resolution).

### 2.2.2. Topographic variables and distance to the coast

We gathered six variables related to topography using raster layers derived from the Global Multi-resolution Terrain Elevation Data 2010 (GMTED2010) dataset at 30 arcsec resolution (Amatulli et al., 2018). Maps on northness and eastness, elevation (m a.s.l.), elevational variation (EleVar) and topographic position index (TPI) were collected. Northness and eastness are the sine of the slope, multiplied by the cosine and sine of the aspect, respectively. They provide continuous measures describing the orientation in combination with the slope (i.e., a circular variable is transformed into a continuous one, ranging from −1 to 1). In the Northern Hemisphere, a northness value close to 1 corresponds to a northern exposition on a vertical slope (i.e., a slope

exposed to very low amount of solar radiation), while a value close to −1 corresponds to a very steep southern slope, exposed to a high amount of solar radiation. Aspect values for the Southern Hemisphere were inverted so that a value of 1 in the Southern Hemisphere also means very low amount of solar radiation. Variables EleVar (1) and TPI (2) capture topographic heterogeneity within a 1 km<sup>2</sup> grid cell around each pair of measurements (inside and outside forest): (1) the standard deviation of elevational values aggregated per 1 km<sup>2</sup> grid cell (further referred to as elevational variation) and (2) the median of the topographic position index (TPI) values across each 1 km<sup>2</sup> grid cell. The TPI is the difference between the elevation of a focal cell and the mean elevation of its eight surrounding cells. Positive and negative values correspond to ridges and valleys, respectively, while zero values correspond to flat areas (Amatulli et al., 2018). We also produced a map with the distance from each land pixel to the nearest coastline (Dist2Coast) using the coastline map data from Natural Earth (free vector data from [naturalearthdata.com](http://naturalearthdata.com)).

### 2.2.3. Forest cover and forest height

We used the tree canopy cover (defined as canopy closure for all vegetation taller than 5 m in height) map for the year 2000 by Hansen et al. (2013). This high-resolution global map layer was re-projected and aggregated from 30 m to 30 arcsec using the average of the aggregated raster cells. This canopy cover map is the only available map spanning a global extent at this high resolution. By using this data product, we make the strong assumption that canopy cover at the time of temperature measurements is similar to the cover in the year 2000. We consider this assumption as reasonable as the median year of the temperature measurements for all data points is approximately 1996 (range between 1943 and 2014). Finally, we used estimates of canopy height at 1 km resolution derived from the ICESat satellite mission based on 2005 (Simard et al., 2011).

## 2.3. Data analysis

All statistical analyses were performed in the open-source statistical software environment of R, version 4.0.2 (R Core Team, 2021). The temperature offsets for  $T_{\text{mean}}$ ,  $T_{\text{max}}$  and  $T_{\text{min}}$  were modelled (274, 184 and 202 plot pairs respectively), after removing missing values for sensor height, i.e. not mentioned in the original study, and data points with canopy cover zero (based on the tree canopy cover map introduced above; Hansen et al., 2013) using linear mixed-effect models with random intercept (LMMs) (*lme4* package; Bates et al., 2015). In our main models, we combined the seasonal (growing vs. non-growing and annual) time series and performed additional analyses for the different three different time periods (see further and Supplementary Material Appendix S2). We included ‘study ID’ as a random intercept term to account for non-independence between samples within studies. For each of the three studied response variables, we started our modelling protocol from the full model:

$$T_{\text{offset}} \sim T_{\text{macro}} + \text{Precipitation} + \text{Elevation} + \text{Eastness} + \text{Northness} \\ + \text{EleVar} + \text{TPI} + \text{Dist2Coast} + \text{Canopy cover} + \text{Forest height} \\ + \text{Sensor height} + \text{random effect 'study ID'}$$

For  $T_{\text{macro}}$ , we used the monthly average for either  $T_{\text{mean}}$ ,  $T_{\text{max}}$  and  $T_{\text{min}}$  temperature during the period 1970–2000 depending on the studied response variable of  $T_{\text{offset}}$  ( $T_{\text{mean}}$ ,  $T_{\text{max}}$  or  $T_{\text{min}}$ ). Sensor height was also included in the models (continuous variable, in metres above or below the soil surface), as this significantly impacts the magnitude of the temperature offset (De Frenne et al., 2019; Supplementary Fig. S2; Table S1). Sensor height is positive for aboveground and negative for belowground sensors. Data points with sensor height > 2 m were excluded as our aim was to model forest microclimate near the ground. To avoid collinearity in predictor variables and improve model performance, we excluded variables that showed a correlation



$r \geq |0.7|$  (Pearson's product-moment correlation; Supplementary Fig. S3) and variance inflation factor  $\geq 4$  (Zuur et al., 2010). Forest height was therefore removed from all models due to high correlation with canopy cover; for  $T_{\text{mean}}$  offset, EleVar was also dropped from the model due to high correlation with TPI. All predictors were standardized by subtracting the mean and dividing by the standard deviation prior to modelling. For each response variable, the single best model was selected based on the Akaike Information Criterion (AIC) using the automated dredge-function of the package MuMIn (Barton, 2009). Goodness of fit was calculated following Nakagawa and Schielzeth (2013).

To test for non-linear relationships, we also used generalized additive mixed-effect models (GAMMs) (cf. the *gamm4* package) (Wood and Scheipl, 2014) on the same dataset. We applied smoothers to the same set of fixed-effect terms, included the same random intercept term 'study ID' and followed the same model selection procedure as for the LMMs. For each of the three studied response variables ( $T_{\text{mean}}$ ,  $T_{\text{max}}$ ,  $T_{\text{min}}$ ) and for each of the two modelling approaches, we performed a leave-one-out cross validation (LOOCv) and compared root mean square errors (RMSE) among models (LMMs vs. GAMMs). We found no difference ( $t$ -test,  $p$ -value  $> 0.05$ ) in RMSE between LMMs and GAMMs, justifying our choice of LMMs (see also Supplementary Fig. S4). Furthermore, we checked spatial autocorrelation in the model residuals for the LMMs using Moran's I-test from the *ape* package (Paradis and Schliep, 2019). No spatial autocorrelation was detected ( $p$ -value  $> 0.05$ ) in the model residuals. Additionally, we tested the effect of season of sampling (annual, growing and non-growing season; see above) on each response variable. We included season as a categorical variable to the full models described above and followed the same model selection procedure. However, due to the low number of observations for each category (but growing season being the dominant category), results including season were only included in the Supplementary Material Appendix S2.

Using the single best LMMs for each of our three response variables, we made predictions for  $T_{\text{mean}}$ ,  $T_{\text{max}}$ , and  $T_{\text{min}}$  offsets for forest across the globe using the collected map data for all predictor variables retained in the models, setting sensor height to 1.0 m and not considering variation included in the random intercept. Temperature offsets were predicted for all raster pixels (30 arcsec resolution) with canopy cover  $> 50\%$  as this largely concurs with the global distribution of forest areas in the terrestrial ecoregions map by Olson et al. (2001). To assess model performance, we performed spatially blocked  $k$ -fold cross-validation ( $k = 10$ ; folds assigned randomly, with spatial blocks of size  $50 \text{ km}^2$ ; Valavi et al., 2019). Furthermore, we made predictions of future forest temperature offsets based on the future projections of temperature and precipitation (the latter only included in the best model for  $T_{\text{mean}}$  and  $T_{\text{min}}$ ) from WorldClim (see above). We made future predictions for the period of 2060–2080 using the RCP 2.6 and RCP 8.5 projections based on the three selected GCMs to account for uncertainty related to the GCMs; final model predictions for each RCP scenario were averaged over all GCMs. For the future predictions, we assumed no change in topography and conservatively assumed no change in canopy cover as our main goal was to determine direct climate change effects on temperature offsets below forest canopies if we maintain the forest cover. Of course, we could use different scenarios of future forest cover but we decided to not do that to better assess the unique effect of future climate change without changing other parameters, such as forest cover, in the model. Besides, future scenario on forest cover are not yet available at a global extent and at the spatial resolution we used here. Uncertainty in predictions was mapped by applying a bootstrap approach. We resampled the original data used to fit the models with replacement with total size of the bootstrap samples equal to the size of the original sample. For each of the temperature responses, we fitted single best models using 30 bootstrap samples. Using these 30 models, we generated per-pixel standard deviation mapped at the global extent (Supplementary Fig. S5). To map uncertainty for the

future predictions, the same procedure was followed for each of the three GCMs, i.e. 30 bootstraps per GCM. Furthermore, we provide maps indicating where the models are extrapolating beyond the values of data used to fit the models. Predictive performance and uncertainty mapping were performed considering fixed effects of the models, excluding uncertainty of the random (study) effects. Predictions were made using the *raster* package (Hijmans and van Etten, 2012). Graphical plots were created using *ggplot2* (Wickham, 2016) and *Tmap* packages (Tennekes, 2018).

### 3. Results

Our models predicted an average global offset of  $-2.92 \pm 1.57^\circ\text{C}$  (mean  $\pm$  SD) for  $T_{\text{max}}$ ,  $-0.88 \pm 1.82^\circ\text{C}$  for  $T_{\text{mean}}$ , and  $0.96 \pm 1.27^\circ\text{C}$  for  $T_{\text{min}}$  (Figs. 1 and 2). These averages were calculated from all pixels having at least 50% canopy cover during the year 2000 (Hansen et al., 2013) and derived from the predictions in Fig. 1. Our predictions show a slightly positive  $T_{\text{mean}}$  offset (i.e. warmer temperatures within the forest) in boreal forests, becoming overall negative towards the tropics (i.e. cooler temperatures within tropical forests compared to free-air temperatures) (left panels Fig. 2).  $T_{\text{max}}$  offsets are negative across the three biomes (i.e. cooler maximum temperatures within forests) with the lowest values in the tropics (up to 5 degrees cooler within forests), whereas  $T_{\text{min}}$  offsets are positive in boreal and temperate forests and negative in the tropics (Fig. 2). When including season in the modelling procedure, we found that for  $T_{\text{mean}}$  offsets were lower during the growing season than for the non-growing season across the three biomes. For  $T_{\text{max}}$  and  $T_{\text{min}}$ , season was not included in the best model (more detailed results included in Supplementary Material Appendix S2).

Offsets for  $T_{\text{max}}$ ,  $T_{\text{mean}}$  and  $T_{\text{min}}$  were negatively affected by free-air, macroclimate temperatures (Supplementary Fig. S2 and Table S1). For  $T_{\text{mean}}$  and  $T_{\text{min}}$ , we found lower offset values with higher amounts of precipitation (Supplementary Fig. S2 and Table S1), for  $T_{\text{mean}}$  this indicates stronger buffering (more negative offsets), whereas for  $T_{\text{min}}$  this means weaker buffering (offsets closer to zero). We found  $T_{\text{min}}$  offsets to be more positive, i.e. more strongly buffered, in areas with higher canopy cover, on pole-facing slopes and closer to the coast. The marginal  $R^2$  values (for fixed effects) were 0.29 (0.03 SD), 0.21 (0.03 SD) and 0.25 (0.03 SD), while conditional  $R^2$  values (for fixed and random effects) reached 0.58 (0.04 SD), 0.60 (0.06 SD) and 0.52 (0.04 SD) for  $T_{\text{max}}$ ,  $T_{\text{mean}}$  and  $T_{\text{min}}$ , respectively. Root mean square errors obtained from the spatial cross-validation were  $3.67^\circ\text{C}$  (1.55 SD),  $1.78^\circ\text{C}$  (0.71 SD) and  $1.52^\circ\text{C}$  (0.45 SD) for  $T_{\text{max}}$ ,  $T_{\text{mean}}$  and  $T_{\text{min}}$ , respectively. Standard deviations obtained from the bootstrapping procedure show fair consistency between the predictions of the 30 bootstrapped models (Supplementary Table S2; Figs. S5 and S6). Upper confidence levels (95%) of standard deviations for all three responses remained lower than  $1^\circ\text{C}$  (Supplementary Table S2 and Fig. S6). Higher values were mainly observed in the tropical and boreal region. We also found higher extrapolation for the predictors included in the models in tropical forests and especially in the boreal region (Supplementary Fig. S7).

Our future projections showed an overall decrease in offset values for all three temperature responses (Fig. 2). For  $T_{\text{mean}}$ , future minus past offsets were  $-0.22 \pm 0.16^\circ\text{C}$  (mean  $\pm$  SD) for RCP2.6 and  $-0.5 \pm 0.22^\circ\text{C}$  for RCP8.5 (Fig. 2). For  $T_{\text{max}}$ , future minus past offsets were  $-0.27 \pm 0.16^\circ\text{C}$  for RCP2.6 and  $-0.60 \pm 0.14^\circ\text{C}$  for RCP8.5 (i.e. cooler maximum temperatures within forests compared to outside temperatures in the future). For  $T_{\text{min}}$ , future minus past offsets were  $-0.12 \pm 0.18^\circ\text{C}$  for RCP2.6 and  $-0.27 \pm 0.24^\circ\text{C}$  for RCP8.5. These averages were derived from panels D, E and F in Fig. 1. For both  $T_{\text{max}}$  and  $T_{\text{mean}}$ , this means stronger offsets or buffering (more negative offsets), whereas for  $T_{\text{min}}$  weaker buffering (offsets closer to zero). Decreases in  $T_{\text{min}}$  offsets are most pronounced in the boreal and temperate region (left panels Fig. 2).

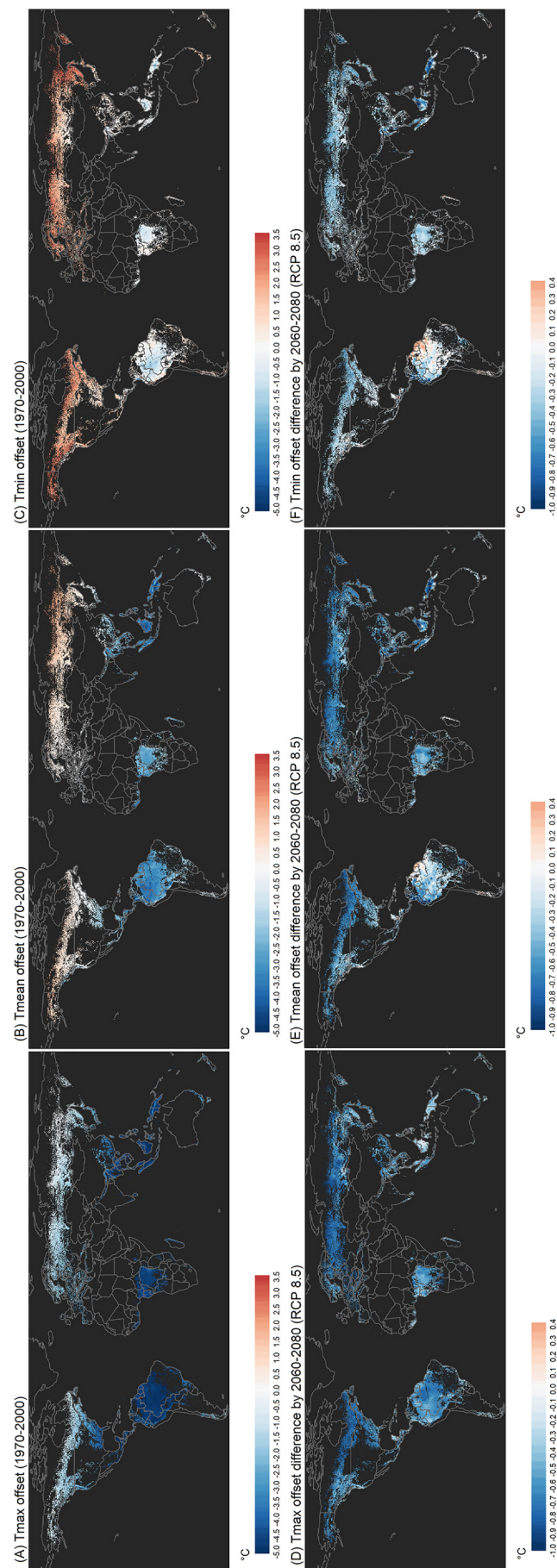


**Fig. 1.** First row: Global maps of past (1970–2000 climate) forest temperature offsets of (A) maximum, (B) mean and (C) minimum temperatures below tree canopies. Second row: Maps showing the difference between (D) maximum, (E) mean and (F) minimum temperature offset predictions based on future climatic conditions under RCP8.5 scenarios and past (1970–2000) offsets (future minus past). Negative values thus depict lower offsets in the future than in the recent past which mean higher buffering for  $T_{max}$  and  $T_{mean}$  but lower for  $T_{min}$ . Predictions were made based on linear mixed-effects models and only for pixels where the canopy cover in the year 2000 is  $>50\%$  (Hansen et al., 2013).

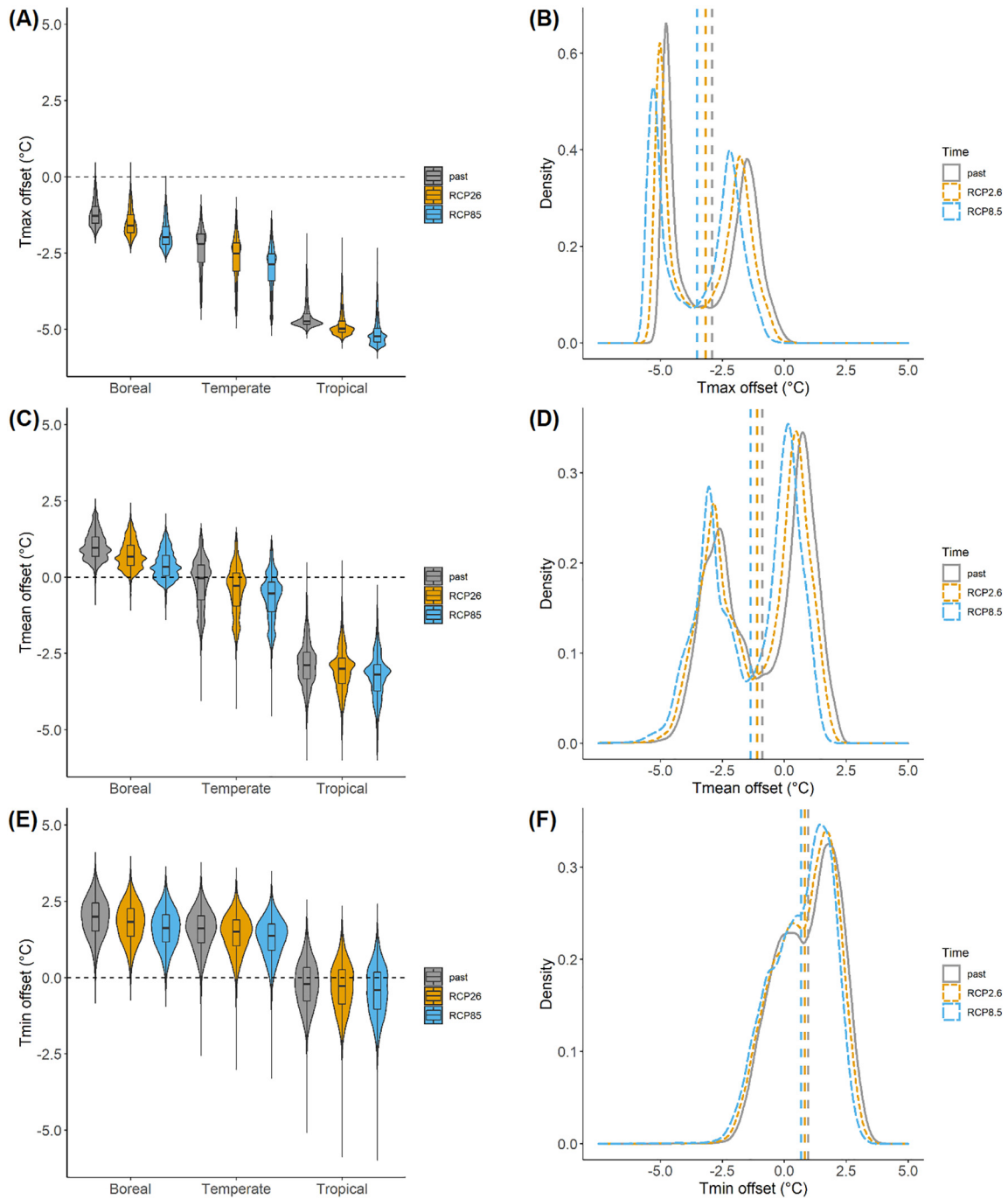


**Fig. 2.** Left panels: Violin and box plots showing the distribution of predicted below-canopy forest temperature offsets of (A)  $T_{\max}$ , (C)  $T_{\text{mean}}$ , and (E)  $T_{\min}$  across boreal, temperate and tropical forests classified following Olson et al. (2001). Right panels: density plots for the predicted offsets of (B)  $T_{\max}$ , (D)  $T_{\text{mean}}$ , and (F)  $T_{\min}$ . Dashed vertical lines represent global mean offset values for the three temperature responses for past, and the future RCP2.6 and RCP8.5 scenarios. Note that bimodality is observed in the density plots, resulting from the difference between offsets in temperate and boreal versus tropical forests (see Fig. 1). For all plots, different colours and line types represent predictions for past climatic conditions (macroclimate temperature and precipitation, grey), for RCP2.6 (orange) and RCP8.5 scenarios (blue). Data points to draw these plots are subsamples ( $10^5$  pixels) derived from the global predictions in Fig. 1.

#### 4. Discussion

Our predictions of temperature offsets for the 1970–2000 climatology and for forests having at least 50% tree cover during the year 2000 (Hansen et al., 2013) show that mean temperatures are on average cooler below canopies (at 1 m height) than in open habitats across all forested grid cells (De Frenne et al., 2019; Li et al., 2015). Our results also support the fact that temperature extremes are mainly buffered

in forests;  $T_{\max}$  is on average lower inside forests, whereas  $T_{\min}$  is warmer. Nevertheless, strong biome-specific variation was observed: while in boreal forests,  $T_{\text{mean}}$  offsets were slightly positive, they became overall negative towards the tropics.  $T_{\max}$  offsets were negative across the three biomes with the most negative values in the (warmer) tropics, whereas  $T_{\min}$  offsets were positive in the cooler boreal and temperate forests, and negative in the warm tropics. Furthermore, the difference between growing and non-growing season



on  $T_{\text{mean}}$  offsets illustrates the importance of considering the temporal and seasonal variation in temperature offsets in future research (Li et al., 2015; Zellweger et al., 2019).

Temperature offsets for all three responses were negatively related to macroclimate temperatures. This relationship is expected as temperature offsets are directly linked to macroclimate temperatures; if free-air temperatures rise, offsets will become more negative because the parameter estimate for  $T_{\text{macro}}$  represents the proportional buffering of canopies of free-air temperatures. Offsets for  $T_{\text{mean}}$  and  $T_{\text{min}}$  were negatively affected by precipitation. That is, the buffering for  $T_{\text{max}}$  by canopies was stronger in regions with higher amounts of precipitation, whereas buffering is lower for  $T_{\text{min}}$ , supporting the notion that evapotranspiration drives the offset in these conditions (Davis et al., 2019). The limited role of drivers other than macroclimate could be because the 30 arcsec (~1 km) spatial resolution is still too coarse to detect effects of e.g. topography or canopy cover, drivers acting on a very local scale (Ashcroft and Gollan, 2012; Greiser et al., 2018; Macek et al., 2019).

Our aim was not to produce maps for use, but to give an overview of how temperature offsets between forest and open habitats vary across forest biomes and how these relationships can evolve under climate change. Despite the limitations of the data and the assumptions made, we found that our models explained a moderately large amount of variation in the offsets, and considered model accuracy to be fair. Uncertainty in predictions increased towards tropical and boreal forests which is likely caused by extrapolation outside the environmental range included in our data. These biomes were underrepresented in the data, hence, future research should focus on setting out networks of paired temperature sensors in these regions (Lembrechts et al., 2021b).

Our projections for both the “very stringent” RCP2.6 as well as the “worst-case” RCP8.5 scenario indicate that buffering by forest canopies for  $T_{\text{mean}}$  and  $T_{\text{max}}$  temperature may increase, but minimum temperature offsets will decrease, especially in temperate and boreal regions as ambient temperatures become less cold. This suggests that under climate change, free-air temperatures are likely to have a larger-magnitude increase than the corresponding forest microclimate temperatures, which would reinforce the idea of divergent warming (decoupling) between macroclimate and microclimate (De Frenne et al., 2019; Lenoir et al., 2017). Offsets may even become lower (resulting in increasing or decreasing buffering for  $T_{\text{mean}}$  or  $T_{\text{min}}$ , respectively) despite projected decreases in precipitation in some regions (Supplementary Fig. S8). It is possible that finer-grained microclimatic heterogeneity could buffer the impact of a changing macroclimate even further (Maclean et al., 2017). This inference relies, however, on the strong assumption that forest cover and composition will remain stable in the future. Such stability is however unlikely, as climate change itself as well as forest management and disturbances can either increase or decrease forest canopy cover in the future. For example, climate change is however likely to cause increased tree mortality owing to, for instance, repeated and more severe disturbances such as droughts, fires, pathogens and insect outbreaks (Curtis et al., 2018; Senf et al., 2021; Senf and Seidl, 2020). The resulting reduction in tree canopy cover can lead to a sudden loss (i.e. a tipping point) of canopy buffering and increased microclimate warming (Alkama and Cescatti, 2016; Findell et al., 2017; Lembrechts and Nijs, 2020; Richard et al., 2021; Zellweger et al., 2020). On the other hand, strong efforts are being made worldwide to increase forest cover and implement climate-smart forestry practices (Bastin et al., 2019; Di Sacco et al., 2021). How these forest cover changes will affect future forest temperature buffering should be a topic for future forest microclimate research.

We projected temperature buffering capacities of forests across the globe under future climate change scenarios. Assuming no change in forest composition, we predicted that forest buffering of  $T_{\text{mean}}$  and  $T_{\text{max}}$  will increase in the future (2060–2080), whereas buffering of  $T_{\text{min}}$  will be reduced due to changes in macroclimate conditions. Our results indicate that the refugial capacity of cool and dense forest

might last longer than anticipated in a warming climate. This knowledge has important implications for forest biodiversity conservation. Forest managers and policymakers could, for example, aim to optimize forest functioning and biodiversity goals by identifying areas in which reducing or retaining canopy cover may have larger impacts on the prevailing microclimate than anticipated under future climate change (Wolf et al., 2021). The paired nature of the data allowed us to model absolute temperature offsets across a global extent with fair accuracy. Gridded microclimate products such as ours, especially when paired with new, well-designed networks of microclimate measurements (Lembrechts et al., 2020) serve ecological and environmental modelers with a more scale-relevant set of products for making predictions and drawing inference. At the regional and even continental scale, novel high-resolution data on forest structure and composition based on remote sensing imagery (e.g. GEDI LiDAR data) are becoming available (De Frenne et al., 2021; Lembrechts et al., 2019; Randin et al., 2020; Zellweger et al., 2018). Including these microclimate measurements and novel spatial map data (e.g. Haesen et al., 2021; Lembrechts et al., 2020) in future models and mapping efforts will increase accuracy of future predictions (Lembrechts et al., 2021a). Our study illustrates that forest microclimates themselves are subject to climate change, which will have important consequences for forest-dwelling species and must hence not be neglected.

## Data availability

The dataset analysed in the current study is available in the Figshare repository, with the identifier <https://doi.org/10.6084/m9.figshare.7604849> (de Frenne et al., 2019).

## CRediT authorship contribution statement

EDL and the participants of the microclimate workshop in Ekenäs 2020 conceived and designed the research. EDL, PDF, FZ, JL, ML, KH and FR-S assembled the data. EDL, PDF, FR-S, KVM, JL and JJJ analysed the data. EDL led the writing of the manuscript with input of all authors.

## Declaration of competing interest

The authors declare that they have no known competing financial interests or personal relationships that could have appeared to influence the work reported in this paper.

## Acknowledgements

EDL, PV, PDF, LD, PS, CM and TV received funding from the European Research Council (ERC) under the European Union's Horizon 2020 research and innovation programme (ERC Starting Grant FORMICA 757833). FZ received funding from the Swiss National Science Foundation (grant number 193645). SH received funding from a FLOF fellowship of the KU Leuven (project nr. 3E190655). Funding for DHK was provided by the National Science Foundation Graduate Research Fellowship Program (DGE-1842473). JA acknowledges Academy of Finland Flagship funding (grant no. 337552). KH received funding from the Swedish Research Council Formas (grants 2014-530 and 2018-2829) and the Bolin Centre for Climate Research, Stockholm University. SG was supported by the Research Foundation Flanders (FWO) (project G0H1517N). JJJ received funding from the Research Foundation Flanders (FWO) (project 12P1819N). JL received funding from the Agence Nationale de la Recherche (ANR) within the framework of the IMPRINT project “Impacts des Processus microclimatiques sur la redistribution de la biodiversité forestière en contexte de réchauffement du macroclimat” (grant number: ANR-19-CE32-0005-01). KDP received funding from the Research Foundation Flanders (FWO) (project ASP035-19). FRS was supported by the VI Plan Propio de Investigación de Universidad de Sevilla (VI PPIT- US).

## Appendix A. Supplementary data

Supplementary data to this article can be found online at <https://doi.org/10.1016/j.scitotenv.2021.151338>.

## References

- Alkama, R., Cescatti, A., 2016. Climate change: biophysical climate impacts of recent changes in global forest cover. *Science* (80-. ) 351, 600–604. <https://doi.org/10.1126/science.aac8083>.
- Amatulli, G., Domisch, S., Tuanmu, M.N., Parmentier, B., Ranipeta, A., Malczyk, J., Jetz, W., 2018. Data descriptor: a suite of global, cross-scale topographic variables for environmental and biodiversity modeling. *Sci. Data* 5, 1–15. <https://doi.org/10.1038/sdata.2018.40>.
- Ashcroft, M.B., Gollan, J.R., 2012. Fine-resolution (25 m) topoclimatic grids of near-surface (5 cm) extreme temperatures and humidities across various habitats in a large (200 × 300 km) and diverse region. *Int. J. Climatol.* 32, 2134–2148. <https://doi.org/10.1002/joc.2428>.
- Barton, K., 2009. *MuMIn: Multi-Model Inference*.
- Bastin, J., Finegold, Y., Garcia, C., Mollicone, D., Rezende, M., Routh, D., Zohner, C., Crowther, T., 2019. The global tree restoration potential. *Science* (80-. ) 365, 76–79. <https://doi.org/10.1126/science.aay8060>.
- Bates, D., Maechler, M., Bolker, B.M., Walker, S., 2015. Fitting linear mixed-effects models using lme4. *J. Stat. Softw.* 67, 1–48. <https://doi.org/10.18637/jss.v067.i01>.
- Chen, J., Saunders, S.C., Crow, T.R., Naiman, R.J., Brososke, K.D., Mroz, G.D., Brookshire, B.L., Franklin, J.F., 1999. Microclimate in forest ecosystem and landscape ecology: variations in local climate can be used to monitor and compare the effects of different management regimes. *Bioscience* 49, 288–297. <https://doi.org/10.2307/1313612>.
- Chen, Y., Liu, Y., Zhang, J., Yang, W., He, R., Deng, C., 2018. Microclimate exerts greater control over litter decomposition and enzyme activity than litter quality in an alpine forest-tundra ecotone. *Sci. Rep.* 8, 1–13. <https://doi.org/10.1038/s41598-018-33186-4>.
- Curtis, P.G., Slay, C.M., Harris, N.L., Tyukavina, A., Hansen, M.C., 2018. Classifying drivers of global forest loss. *Science* (80-. ) 361, 1108–1111. <https://doi.org/10.1126/science.aau3445>.
- Davis, K.T., Dobrowski, S.Z., Holden, Z.A., Higuera, P.E., Abatzoglou, J.T., 2019. Microclimatic buffering in forests of the future: the role of local water balance. *Ecography* (Cop.) 42, 1–11. <https://doi.org/10.1111/ecog.03836>.
- De Frenne, P., Rodríguez-Sánchez, F., Coomes, D.A., Baeten, L., Verstraeten, G., Vellend, M., Bernhardt-Römermann, M., Brown, C.D., Brunet, J., Cornelis, J., Decocq, G.M., Dierschke, H., Eriksson, O., Gilliam, F.S., Hédli, R., Heinken, T., Hermy, M., Hommel, P., Jenkins, M.A., Kelly, D.L., Kirby, K.J., Mitchell, F.J.G., Naaf, T., Newman, M., Peterken, G., Petrik, P., Schultz, J., Sonnier, G., Van Calster, H., Waller, D.M., Walther, G.-R., White, P.S., Woods, K.D., Wulf, M., Graae, B.J., Verheyen, K., 2013. Microclimate moderates plant responses to macroclimate warming. *Proc. Natl. Acad. Sci. U. S. A.* 110, 18561–18565. <https://doi.org/10.1073/pnas.1311190110>.
- De Frenne, P., Zellweger, F., Rodríguez-Sánchez, F., Scheffers, B.R., Hylander, K., Luoto, M., Vellend, M., Verheyen, K., Lenoir, J., 2019. Global buffering of temperatures under forest canopies. *Nat. Ecol. Evol.* 3, 744–749. <https://doi.org/10.1038/s41559-019-0842-1>.
- De Frenne, P., Lenoir, J., Luoto, M., Scheffers, B.R., Zellweger, F., Aalto, J., Ashcroft, M.B., Christiansen, D.M., Decocq, G., Pauw, K.D., Govaert, S., Greiser, C., Gril, E., Hampe, A., Jucker, T., Klimes, D.H., Koelemeijer, I.A., Lembrechts, J.J., Marrec, R., Meeussen, C., Ogée, J., Tyystjärvi, V., Vangansbeke, P., Hylander, K., 2021. Forest microclimates and climate change: importance, drivers and future research agenda. *Glob. Chang. Biol.* 1–19. <https://doi.org/10.1111/gcb.15569>.
- De Smedt, P., Boeraeve, P., Baeten, L., 2021. Intra-annual activity patterns of terrestrial isopods are tempered in forest compared to open habitat. *Soil Biol. Biochem.* 160, 108342. <https://doi.org/10.1016/j.soilbio.2021.108342>.
- Di Sacco, A., Hardwick, K.A., Blakesley, D., Brancalion, P.H.S., Berman, E., Cecilio Rebola, L., Chomba, S., Dixon, K., Elliott, S., Ruyonga, G., Shaw, K., Smith, P., Smith, R.J., Antonelli, A., 2021. Ten golden rules for reforestation to optimize carbon sequestration, biodiversity recovery and livelihood benefits. *Glob. Chang. Biol.* 27, 1328–1348. <https://doi.org/10.1111/gcb.15498>.
- Dietz, L., Collet, C., Dupouey, J.L., Lacombe, E., Laurent, L., Gégout, J.C., 2020. Windstorm-induced canopy openings accelerate temperate forest adaptation to global warming. *Glob. Ecol. Biogeogr.* 2067–2077. <https://doi.org/10.1111/geb.13177>.
- Fick, S.E., Hijmans, R.J., 2017. WorldClim 2: new 1-km spatial resolution climate surfaces for global land areas. *Int. J. Climatol.* 37, 4302–4315. <https://doi.org/10.1002/joc.5086>.
- Findell, K.L., Berg, A., Gentine, P., Krasting, J.P., Lintner, B.R., Malyshev, S., Santanello, J.A., Shevliakova, E., 2017. The impact of anthropogenic land use and land cover change on regional climate extremes. *Nat. Commun.* 8, 1–9. <https://doi.org/10.1038/s41467-017-01038-w>.
- de Frenne, P., Lenoir, J., Rodríguez-Sánchez, F., 2019. Global buffering of temperatures under forest canopies data and code. Figshare <https://doi.org/10.6084/m9.figshare.7604849tem>.
- Frey, S.J.K., Hadley, A.S., Betts, M.G., 2016a. Microclimate predicts within-season distribution dynamics of montane forest birds. *Divers. Distrib.* 22, 944–959. <https://doi.org/10.1111/ddi.12456>.
- Frey, S.J.K., Hadley, A.S., Johnson, S.L., Schulze, M., Jones, J.A., Betts, M.G., 2016b. Spatial models reveal the microclimatic buffering capacity of old-growth forests. *Sci. Adv.* 2, <https://doi.org/10.1126/sciadv.1501392>.
- Geiger, R., Aron, R., Todhunter, P., 2009. *The climate near the ground*. Rowman & Littlefield.
- Greiser, C., Meineri, E., Luoto, M., Ehrlén, J., Hylander, K., 2018. Monthly microclimate models in a managed boreal forest landscape. *Agric. For. Meteorol.* 250–251, 147–158. <https://doi.org/10.1016/j.agrformet.2017.12.252>.
- Haesen, S., Lembrechts, J.J., De Frenne, P., Lenoir, J., Aalto, J., Ashcroft, M.B., Kopecký, M., Luoto, M., Maclean, I., Nijs, I., Niittynen, P., Hoogen, J., Arriga, N., Bruna, J., Buchmann, N., Čiliak, M., Collalti, A., De Lombaerde, E., Descombes, P., Gharun, M., Gode, I., Govaert, S., Greiser, C., Grelle, A., Gruening, C., Hederová, L., Hylander, K., Kreyling, J., Kruijt, B., Macek, M., Máliš, F., Man, M., Manca, G., Matula, R., Meeussen, C., Merinero, S., Minerbi, S., Montagnani, L., Muffler, L., Ogaya, R., Penuelas, J., Plichta, R., Portillo-Estrada, M., Schmeddes, J., Shekhar, A., Spicher, F., Ujházyová, M., Vangansbeke, P., Weigel, R., Wild, J., Zellweger, F., Van Meerbeek, K., 2021. ForestTemp – sub-canopy microclimate temperatures of European forests. *Glob. Chang. Biol.* 1–13. <https://doi.org/10.1111/gcb.15892>.
- Hansen, M.C., Potapov, P.V., Moore, R., Hancher, M., Turubanova, S.A., Tyukavina, A., Thau, D., Stehman, S.V., Goetz, S.J., Loveland, T.R., Kommareddy, A., Egorov, A., Chini, L., Justice, C.O., Townshend, J.R.G., 2013. High-resolution global maps of 21st-century forest cover change. *Science* (80-. ) 342, 850–854. <https://doi.org/10.1126/science.1244693>.
- Hijmans, R.J., van Etten, J., 2012. *raster: Geographic analysis and modeling with raster data*.
- IPCC, 2018. *Global Warming of 1.5 °C – SR15 – Summary for Policy Makers*, IPCC Climate Change Synthesis Report.
- Lembrechts, J.J., Nijs, I., 2020. Microclimate shifts in a dynamic world. *Science* (80-. ) 368, 711–712.
- Lembrechts, J.J., Nijs, I., Lenoir, J., 2019. Incorporating microclimate into species distribution models. *Ecography* (Cop.) 42, 1267–1279. <https://doi.org/10.1111/ecog.03947>.
- Lembrechts, J.J., Aalto, J., Ashcroft, M.B., De Frenne, P., Kopecký, M., Lenoir, J., Luoto, M., Maclean, I.M.D., Rouspard, O., Fuentes-Lillo, E., García, R.A., Pellissier, L., Pitteloud, C., Alatalo, J.M., Smith, S.W., Björk, R.G., Muffler, L., Ratier Backes, A., Cesarz, S., Gottschall, F., Okello, J., Urban, J., Plichta, R., Svátek, M., Phartyal, S.S., Wipf, S., Eisenhauer, N., Puşcaş, M., Turtureanu, P.D., Varlagin, A., Dimarco, R.D., Jump, A.S., Randall, K., Dorrepaal, E., Larson, K., Walz, J., Vitale, L., Svoboda, M., Finger Higgins, R., Halbritter, A.H., Curasi, S.R., Klupar, I., Koontz, A., Pearce, W.D., Simpson, E., Stenkovski, M., Jessen Graae, B., Vedel Sørensen, M., Høye, T.T., Fernández Calzado, M.R., Lorite, J., Carbognani, M., Tomaselli, M., Forte, T.G.W., Petraglia, A., Haesen, S., Somers, B., Van Meerbeek, K., Björkman, M.P., Hylander, K., Merinero, S., Gharun, M., Buchmann, N., Dolezal, J., Matula, R., Thomas, A.D., Bailey, J.J., Ghosn, D., Kazakis, G., de Pablo, M.A., Kemppinen, J., Niittynen, P., Rew, L., Seipel, T., Larson, C., Speed, J.D.M., Ardó, J., Cannone, N., Guglielmin, M., Malfasi, F., Bader, M.Y., Canessa, R., Stanisci, A., Kreyling, J., Schmeddes, J., Teuber, L., Ascherio, V., Čiliak, M., Máliš, F., De Smedt, P., Govaert, S., Meeussen, C., Vangansbeke, P., Gigauri, K., Lamprecht, A., Pauli, H., Steinbauer, K., Winkler, M., Ueyama, M., Nuñez, M.A., Ursu, T.M., Haider, S., Wedegärtner, R.E.M., Smiljanic, M., Trouillier, M., Wilmking, M., Altman, J., Bruna, J., Hederová, L., Macek, M., Man, M., Wild, J., Vittoz, P., Pärtel, M., Barančok, P., Kanka, R., Kollár, J., Palaj, A., Barros, A., Mazzolari, A.C., Batters, M., Boeckx, P., Benito Alonso, J.L., Zong, S., Di Cecco, V., Sitková, Z., Tielbörger, K., van den Brink, L., Weigel, R., Homeier, J., Dahlberg, C.J., Medinets, S., Medinets, V., De Boeck, H.J., Portillo-Estrada, M., Verryck, L.T., Milbau, A., Daskalova, G.N., Thomas, H.J.D., Myers-Smith, I.H., Blonder, B., Stephan, J.G., Descombes, P., Zellweger, F., Frei, E.R., Heinesch, B., Andrews, C., Dick, J., Siebicke, L., Rocha, A., Senior, R.A., Rixen, C., Jimenez, J.J., Boike, J., Pauchard, A., Scholten, T., Scheffers, B., Klimes, D., Basham, E.W., Zhang, J., Zhang, Z., Géron, C., Fazlioglu, F., Candan, O., Sallo Bravo, J., Hrbacek, F., Laska, K., Cremonese, E., Haase, P., Moyano, F.E., Rossi, C., Nijs, I., 2020. SoilTemp: a global database of near-surface temperature. *Glob. Chang. Biol.* 26, 6616–6629. <https://doi.org/10.1111/gcb.15123>.
- Lembrechts, J.J., Van Den Hoogen, J., Aalto, J., Ashcroft, M.B., De Frenne, P., Kemppinen, J., Kopecký, M., 2021a. Mismatches between soil and air temperature. *EcoEvoRxiv* <https://doi.org/10.32942/osf.io/pksqw>.
- Lembrechts, J.J., Lenoir, J., Frenne, P., De Scheffers, B.R., 2021b. Designing countrywide and regional microclimate networks, pp. 1–7. <https://doi.org/10.1111/gcb.13290>.
- Lenoir, J., Hattab, T., Pierre, G., 2017. Climatic microrefugia under anthropogenic climate change: implications for species redistribution. *Ecography* (Cop.) 40, 253–266. <https://doi.org/10.1111/ecog.02788>.
- Li, Y., Zhao, M., Motesharrei, S., Mu, Q., Kalnay, E., Li, S., 2015. Local cooling and warming effects of forests based on satellite observations. *Nat. Commun.* 6. <https://doi.org/10.1038/ncomms7603>.
- Macek, M., Kopecký, M., Wild, J., 2019. Maximum air temperature controlled by landscape topography affects plant species composition in temperate forests. *Landsc. Ecol.* 34, 2541–2556. <https://doi.org/10.1007/s10980-019-00903-x>.
- Maclean, I.M.D., Suggett, A.J., Wilson, R.J., Duffy, J.P., Bennie, J.J., 2017. Fine-scale climate change: modelling spatial variation in biologically meaningful rates of warming. *Glob. Chang. Biol.* 23, 256–268. <https://doi.org/10.1111/gcb.13343>.
- Nakagawa, S., Schielzeth, H., 2013. A general and simple method for obtaining R<sup>2</sup> from generalized linear mixed-effects models. *Methods Ecol. Evol.* 4, 133–142. <https://doi.org/10.1111/j.2041-210x.2012.00261.x>.
- Olson, D.M., Dinerstein, E., Wikramanayake, E.D., Burgess, N.D., Powell, G.V.N., Underwood, E.C., Amico, J.A.D., Itoua, I., Strand, H.E., Morrison, J.C., Loucks, J., Allnutt, T.F., Ricketts, T.H., Kura, Y., Lamoreux, J.F., Wesley, W., Hedao, P., Kassem, K.R., 2001. *Terrestrial Ecoregions of the World: A New Map of Life on Earth*. 51, pp. 933–938.
- Paradis, E., Schliep, K., 2019. Ape 5.0: an environment for modern phylogenetics and evolutionary analyses in R. *Bioinformatics* 35, 526–528. <https://doi.org/10.1093/bioinformatics/bty633>.
- R Core Team, 2021. *R: a language and environment for statistical computing*.
- Randin, C.F., Ashcroft, M.B., Bolliger, J., Cavender-Bares, J., Coops, N.C., Dullinger, S., Dirnböck, T., Eckert, S., Ellis, E., Fernández, N., Giuliani, G., Guisan, A., Jetz, W., Joost,



- S., Karger, D., Lembrechts, J., Lenoir, J., Luoto, M., Morin, X., Price, B., Rocchini, D., Schaepman, M., Schmid, B., Verburg, P., Wilson, A., Woodcock, P., Yoccoz, N., Payne, D., 2020. Monitoring biodiversity in the anthropocene using remote sensing in species distribution models. *Remote Sens. Environ.* 239, 111626. <https://doi.org/10.1016/j.rse.2019.111626>.
- Richard, B., Dupouey, J.L., Corcket, E., Alard, D., Archaux, F., Aubert, M., Boulanger, V., Gillet, F., Langlois, E., Macé, S., Montpied, P., Beaufils, T., Begeot, C., Behr, P., Boissier, J.M., Camaret, S., Chevalier, R., Decocq, G., Dumas, Y., Eynard-Machet, R., Gégout, J.C., Huet, S., Malécot, V., Margerie, P., Mouly, A., Paul, T., Renaux, B., Ruffaldi, P., Spicher, F., Thirion, E., Ulrich, E., Nicolas, M., Lenoir, J., 2021. The climatic debt is growing in the understorey of temperate forests: stand characteristics matter. *Glob. Ecol. Biogeogr.* 30, 1474–1487. <https://doi.org/10.1111/geb.13312>.
- Sanderson, B.M., Knutti, R., Caldwell, P., 2015. A representative democracy to reduce interdependency in a multimodel ensemble. *J. Clim.* 28, 5171–5194. <https://doi.org/10.1175/JCLI-D-14-00362.1>.
- Senf, C., Seidl, R., 2020. Mapping the forest disturbance regimes of Europe. *Nat. Sustain.* <https://doi.org/10.1038/s41893-020-00609-y>.
- Senf, C., Sebal, J., Seidl, R., 2021. Increasing canopy mortality affects the future demographic structure of Europe's forests. *One Earth* 1–7. <https://doi.org/10.1016/j.oneear.2021.04.008>.
- Simard, M., Pinto, N., Fisher, J.B., Baccini, A., 2011. Mapping forest canopy height globally with spaceborne lidar. *J. Geophys. Res. Biogeosciences* 116, 1–12. <https://doi.org/10.1029/2011JG001708>.
- Stevens, J.T., Safford, H.D., Harrison, S., Latimer, A.M., 2015. Forest disturbance accelerates thermophilization of understory plant communities. *J. Ecol.* 103, 1253–1263. <https://doi.org/10.1111/1365-2745.12426>.
- Tennekes, M., 2018. Tmap: thematic maps in R. *J. Stat. Softw.* 84. <https://doi.org/10.18637/jss.v084.i06>.
- Thrippleton, T., Bugmann, H., Kramer-Priewasser, K., Snell, R.S., 2016. Herbaceous understorey : an overlooked player in forest landscape dynamics? *Ecosystems* 19, 1240–1254. <https://doi.org/10.1007/s10021-016-9999-5>.
- Valavi, R., Elith, J., Lahoz-Monfort, J.J., Guillerá-Arroita, G., 2019. blockCV: an r package for generating spatially or environmentally separated folds for k-fold cross-validation of species distribution models. *Methods Ecol. Evol.* 10, 225–232. <https://doi.org/10.1111/2041-210X.13107>.
- Von Arx, G., Graf Pannatier, E., Thimonier, A., Rebetez, M., 2013. Microclimate in forests with varying leaf area index and soil moisture: potential implications for seedling establishment in a changing climate. *J. Ecol.* 101, 1201–1213. <https://doi.org/10.1111/1365-2745.12121>.
- Wickham, H., 2016. *ggplot2: Elegant graphics for data analysis*. Springer, New York, USA.
- Wolf, C., Bell, D.M., Kim, H., Paul, M., Schulze, M., Betts, M.G., Northwest, P., <collab>Service, U.F.</collab>, Way, S.W.J., Or, C., 2021. Temporal consistency of undercanopy thermal refugia in old-growth forest. *Agric. For. Meteorol.* 307, 108520. <https://doi.org/10.1016/j.agrformet.2021.108520>.
- Wood, S., Scheipl, F., 2014. *gamm4: Generalized additive mixed models using mgcv and lme4*.
- World Meteorological Organization, 2018. *Guide to meteorological instruments and methods of observation*. 2018 ed. WMO.
- Zellweger, F., De Frenne, P., Lenoir, J., Rocchini, D., Coomes, D., 2018. Advances in microclimate ecology arising from remote sensing. *Trends Ecol. Evol.* xx, 1–15. <https://doi.org/10.1016/j.tree.2018.12.012>.
- Zellweger, F., Coomes, D., Lenoir, J., Depauw, L., Maes, S.L., Wulf, M., Kirby, K.J., Brunet, J., Kopecký, M., Máliš, F., Schmidt, W., Heinrichs, S., den Ouden, J., Jaroszewicz, B., Buyse, G., Spicher, F., Verheyen, K., De Frenne, P., 2019. Seasonal drivers of understorey temperature buffering in temperate deciduous forests across Europe. *Glob. Ecol. Biogeogr.* 28, 1774–1786. <https://doi.org/10.1111/geb.12991>.
- Zellweger, F., De Frenne, P., Lenoir, J., Vangansbeke, P., Verheyen, K., Bernhardt-römermann, M., Baeten, L., Hédli, R., Berki, I., Brunet, J., Van Calster, H., Chudomelov, 2020. Forest microclimate dynamics drive plant responses to warming. *Science* (80-. ) 368, 772–775.
- Zuur, A.F., Ieno, E.N., Elphick, C.S., 2010. A protocol for data exploration to avoid common statistical problems, pp. 3–14 <https://doi.org/10.1111/j.2041-210X.2009.00001.x>.